EFFICIENT HIGH-ENERGY HCl CHEMICAL LASER

MATHEMATICAL SCIENCES NORTHWEST, INCORPORATED

PREPARED FOR
OFFICE OF NAVAL RESEARCH

15 NOVEMBER 1975

Second Semi-Annual Report

EFFICIENT HIGH-ENERGY HCl CHEMICAL LASER

MATHEMATICAL SCIENCES NORTHWEST, INC.
P.O. BOX 1887 BELLEVUE, WASHINGTON 98009

Second Semi-Annual Report

EFFICIENT HIGH-ENERGY HCl CHEMICAL LASER

by

Leonard Y. Nelson
and
Stanley R. Byron

MATHEMATICAL SCIENCES NORTHWEST, INC.
P. O. Box 1887
Bellevue, Washington 98009

November 15, 1975

Contract N00014-75-C-0052

Sponsored by
Advanced Research Projects Agency
ARPA Order No. 1807

Monitored by
Office of Naval Research
Code 421

UNCLASSIFIED

SECURITY CLASSIFICATION OF THIS PAGE (When Data Entered)

REPORT DOCUMENTATION PAGE		READ INSTRUCTIONS BEFORE COMPLETING FORM
1. REPORT NUMBER 75-131-2	2. GOVT ACCESSION NO.	3. RECIPIENT'S CATALOG NUMBER
4. TITLE (and Subtitle) Efficient High-Energy HCl Chemical Laser		5. TYPE OF REPORT & PERIOD COVERED Semi-Annual 15 Jan.1975 - 15 July 1975
		6. PERFORMING ORG. REPORT NUMBER MSNW 75-131-2
7. AUTHOR(s) Leonard Y. Nelson and Stanley R. Byron		8. CONTRACT OR GRANT NUMBER(s) N00014-75-C-0052
9. PERFORMING ORGANIZATION NAME AND ADDRESS Mathematical Sciences Northwest, Inc. P. O. Box 1887 Bellevue, Washington 98009		10. PROGRAM ELEMENT, PROJECT, TASK AREA & WORK UNIT NUMBERS
11. CONTROLLING OFFICE NAME AND ADDRESS		12. REPORT DATE November 15, 1975
		13. NUMBER OF PAGES 43
14. MONITORING AGENCY NAME & ADDRESS(if different from Controlling Office) Office of Naval Research 800 North Quincy Street Arlington, Virginia 22217		15. SECURITY CLASS. (of this report) Unclassified
		15a. DECLASSIFICATION/DOWNGRADING SCHEDULE

16. DISTRIBUTION STATEMENT (of this Report)

17. DISTRIBUTION STATEMENT (of the abstract entered in Block 20, if different from Report)

18. SUPPLEMENTARY NOTES

19. KEY WORDS (Continue on reverse side if necessary and identify by block number)

HCl Laser
Vibrational Rate Enhancement
Coherent Anti-Stokes Raman Scattering
Cold Cathode Electron Gun

20. ABSTRACT (Continue on reverse side if necessary and identify by block number)

Further improvements in electrical efficiency have been obtained in the HCl chemical laser using a higher current cold cathode electron gun. HCl laser energies of 1.2 J/ℓ-atm at 4 percent electrical efficiency were achieved. There is a strong indication that shorter pulse durations would be desirable and modifications to the apparatus are currently underway to produce shorter pulse, higher current operation. The HCl laser energy increased four fold when discharge excitation was added to the electron beam excitation.

DD FORM 1 JAN 73 1473 EDITION OF 1 NOV 65 IS OBSOLETE

UNCLASSIFIED

SECURITY CLASSIFICATION OF THIS PAGE (When Data Entered)

20. Abstract - continued

It has not yet been possible to identify the mechanism responsible for the increased laser output associated with discharge excitation; vibrational excitation of H_2, and additional atom production are the most likely possibilities. Successful operation of the hydrogen diagnostic equipment (CARS spectroscopy) has been demonstrated and will be applied to explore the role of $H_2(v)$ in the reaction kinetics.

TABLE OF CONTENTS

LIST OF TABLES

LIST OF FIGURES

SECTION I

SUMMARY

The goal of this program is to utilize vibrational excitation of H_2 to speed up the chemical reaction between H_2 and Cl_2 and thereby provide an efficient, high-energy HCl chemical laser. During the previous reporting period (Ref. 1), experiments clearly showed enhancement in laser output by electrical excitation of the gas mixture. However the high electron attachment rate of Cl_2 prevented high energy densities from being realized at the limited electron beam current density available (50 mamp/cm^2). Considerable increase in HCl laser energy output has been realized in the present reporting period by using a high current, long pulse cold cathode electron gun (0.2 amp/cm^2 for 10 μsec). HCl laser output energies in excess of 1 J/ℓ-atm have been obtained. As in the case of the lower e-beam current density experiments performed with the five tube plasma diode device, application of a discharge voltage significantly enhanced the laser output energy. There is a strong trend in the present data which suggests that even higher e-beam current densities and shorter discharge pulse durations would considerably improve the laser performance. Modifications to the apparatus are currently underway to achieve a significantly higher e-beam current density (> 2 amps/cm^2) and shorter ($\leq$ 1 μsec) discharge pulse.

Spectroscopic methods for measuring the Cl_2 concentration, HCl(V) populations and the extent of H_2 vibrational excitation have been tested. The Coherent Anti-Stokes Raman Scattering (CARS) approach for measuring H_2(V) has been shown to be a viable technique. The Cl_2 optical absorption technique has also been tested, and a brighter, perhaps coherent, light

source is currently being sought to improve the detectivity levels. An HCl probe laser has been operated under conditions needed to avoid line shift problems relative to the experimental laser conditions.

A computer model for the HCl chemical laser has been formulated and the essential rate constants have been tabulated. The actual programming of the computer model will be completed shortly.

SECTION II

HCl LASER PERFORMANCE IN THE COLD CATHODE ELECTRON GUN

The design characteristics of the cold cathode electron gun were described in Reference 1; the operating characteristics measured during the present reporting period are presented here in Section 2.1. In addition, HCl laser performance and discharge characteristics were studied using the cold cathode electron gun facility and these results are presented in Section 2.2. A discussion of the experimental results is given in Section 2.3.

2.1 Electron Beam Operating Conditions

A preliminary description of the cold cathode electron gun and its long pulse characteristics were given in Reference 1. Figure 1 shows how the electron current density of the device depends upon the internal anode-cathode spacing and the voltage applied to the cathode. The current density was measured using the discharge anode as a collector and a Pearson probe enclosing a shorting lead from the anode to the ground. The current pulse duration measured by the Pearson probe as a function of the internal gun spacing is shown in Figure 2. Uniformity of the electron beam source was measured using thin blue cellophane plastic as a dosimeter; for all values of the internal gun spacing, the current density 1 cm from the e-beam foil window was essentially uniform over the full window aperture. Figure 3 shows the measured discharge current in an $Ar/H_2/Cl_2$ (49.5/49.5/1) mixture at fixed E/N (2.8×10^{-16} V-cm^2) as a function of the internal gun spacing and e-beam voltage. The discharge currents are proportional to the e-beam current density (Fig. 1) divided by the gun voltage, as expected for an attachment dominated discharge.

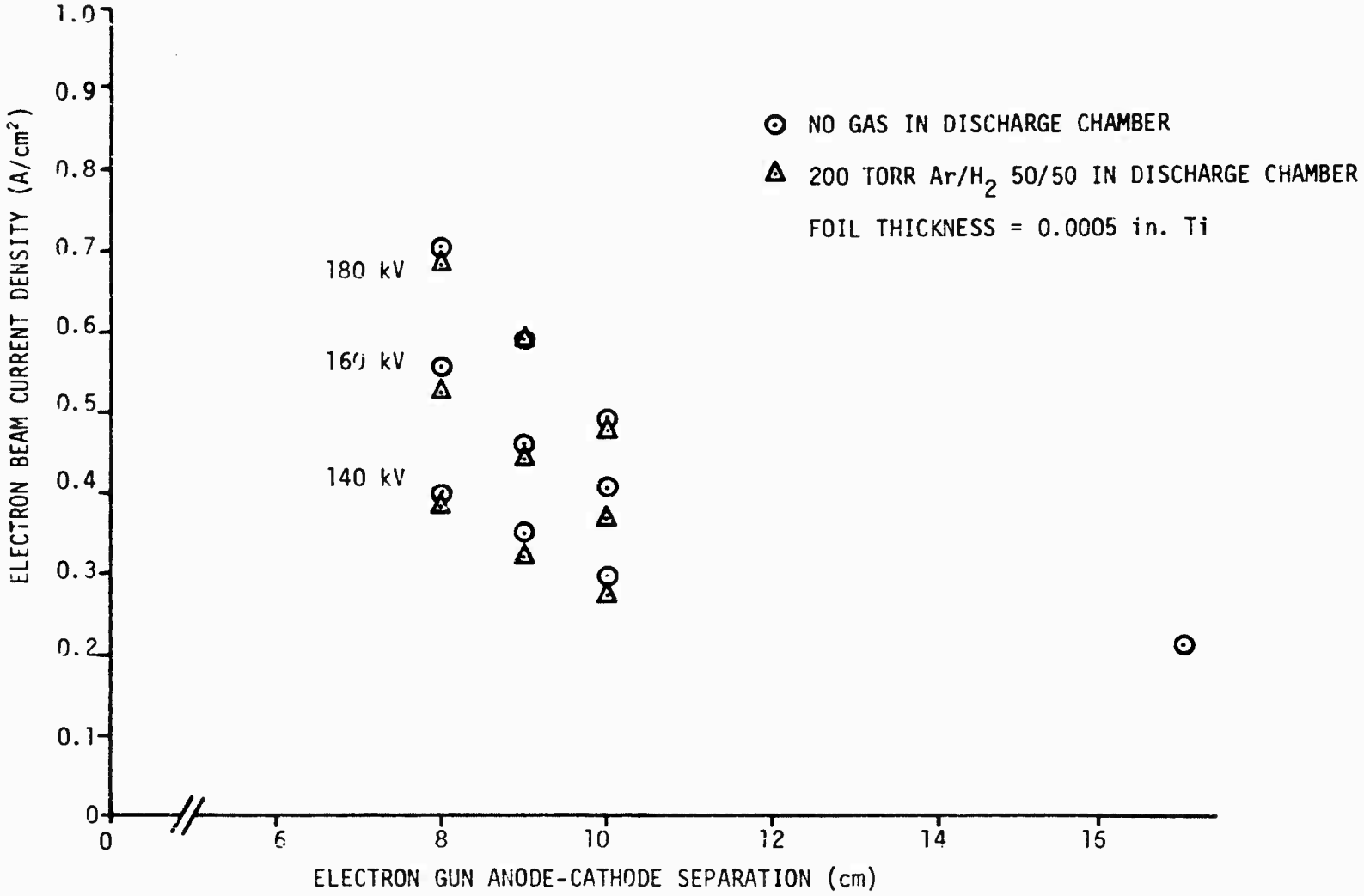

Figure 1. Electron Beam Current Density vs. Anode-Cathode Separation

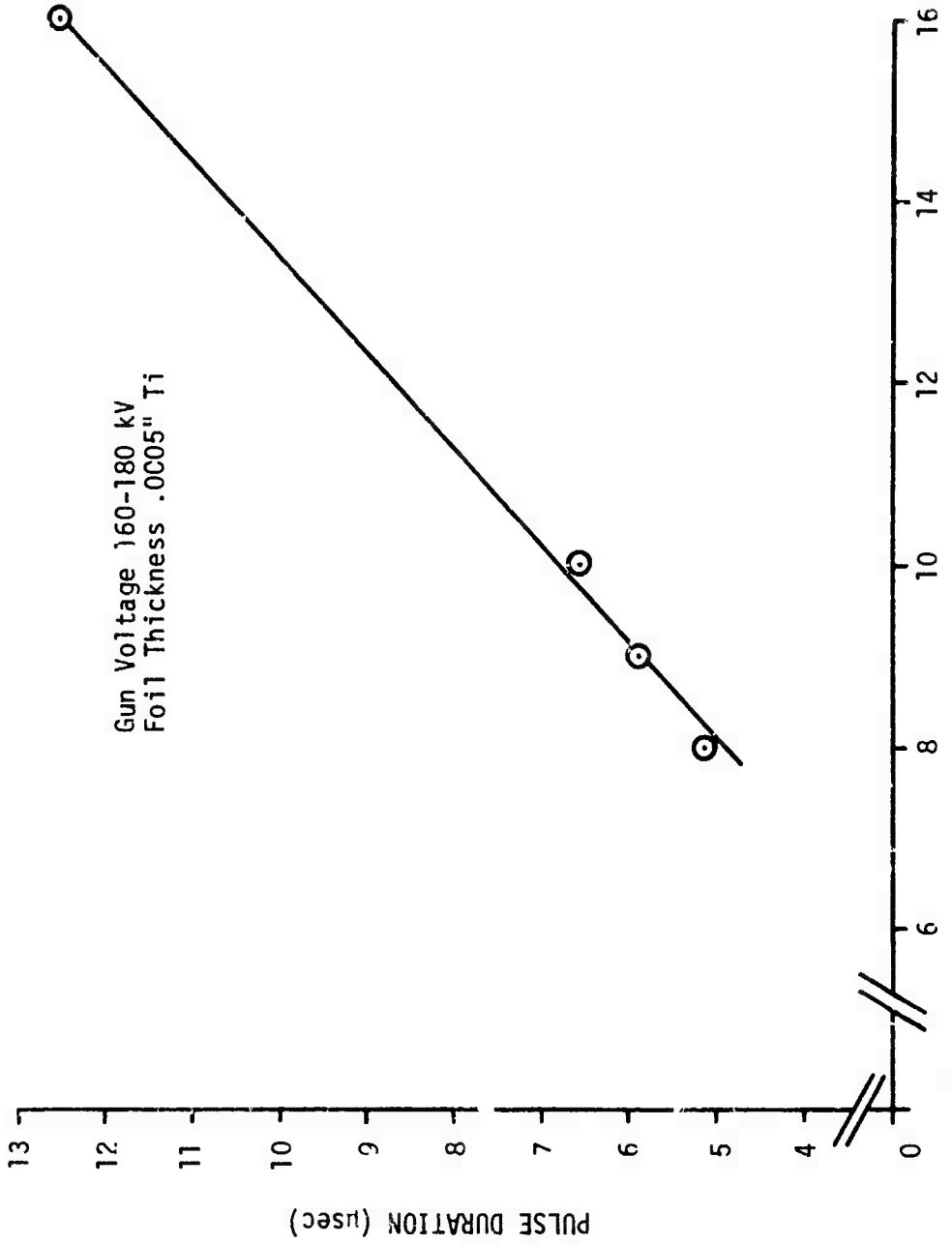

Figure 2. Electron Beam Pulse Duration vs. Anode-Cathode Separation

76 00082

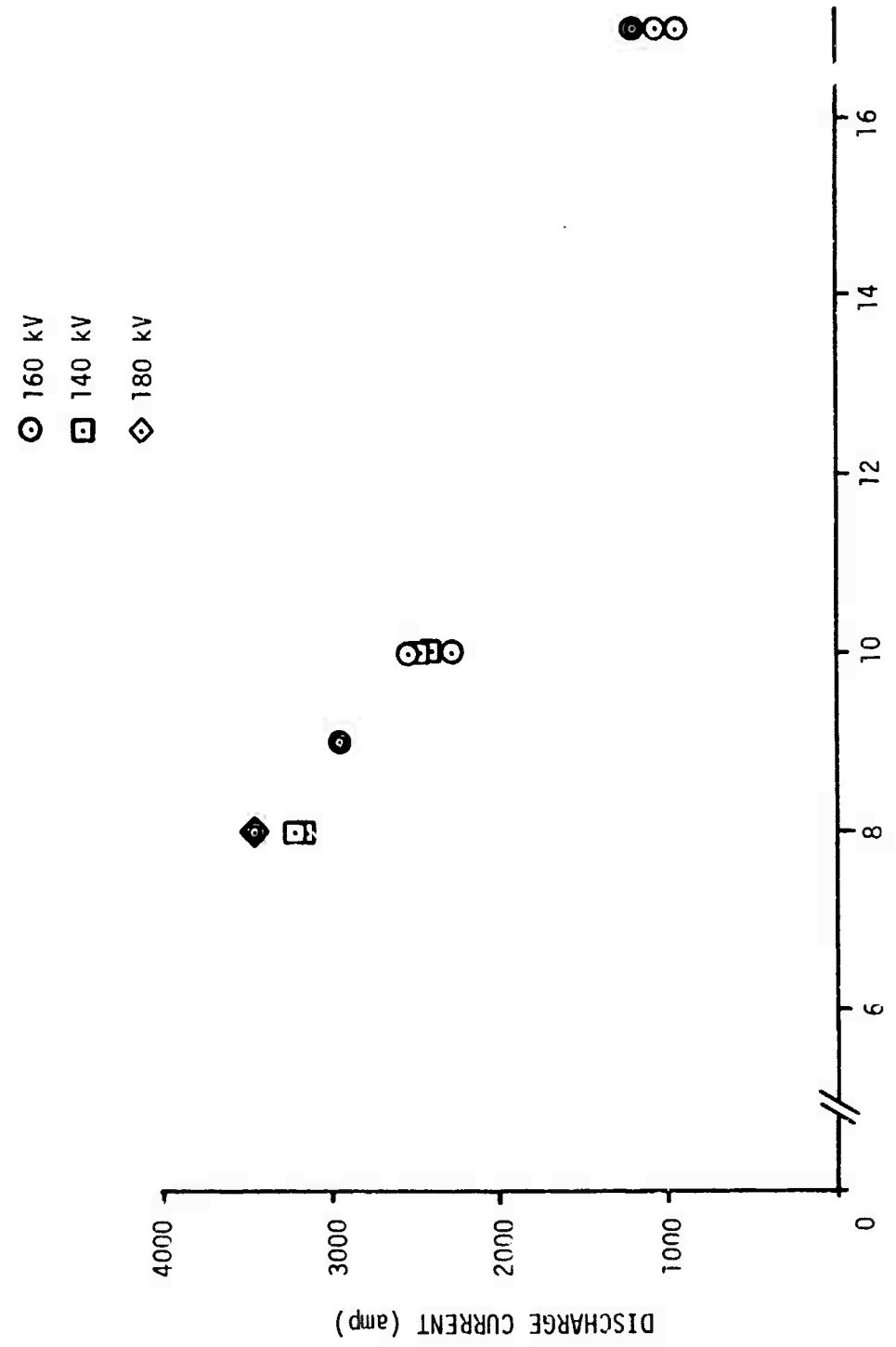

Figure 3. Discharge Current vs Anode-Cathode Separation

76 00083

Since the electron beam is emitted over the full foil window aperture (10 x 50 cm^2), the discharge may not be limited to the 5 cm discharge anode width. Hence the true discharge current density may be somewhat lower than that calculated by dividing the total discharge current by the discharge anode area (240 cm^2). A limiting aperture will be placed in front of the e-beam window in future experiments to remove any possible ambiguities.

2.2. Parametric Laser Performance Studies

2.2.1. Gas Sample Preparation and Composition

Argon, hydrogen, and chlorine mixtures were allowed to flow into the discharge chamber using flow meters and needle valves to adjust the relative concentrations. Following a 10 second purge, the exhaust valve of the discharge chamber was closed and the total pressure raised to the desired value. Following every discharge shot, the entire discharge chamber was evacuated to approximately 1 torr prior to beginning the refill purge.

$Ar/H_2/Cl_2$ gas mixtures were typically 1 to 2 percent Cl_2, with the remainder consisting of equal amounts of argon and hydrogen. Gas pressures of 100 to 250 torr were investigated and it was found that 200 torr was optimum.

2.2.2. Laser Performance Summary

Table I presents a performance summary for the HCl laser under the most optimum conditions found to date (see Fig. 4b). Addition of the sustainer voltage increased the laser output by a factor of four; however,

Table I

HCl Chemical Laser Performance

$Ar/H_2/Cl_2$ 49/49/2; P_{total} = 200 torr

EXPERIMENTAL OBSERVATIONS	E-BEAM	E-BEAM PLUS SUSTAINER
Energy Input (J/ℓ-atm)	4.8	314.8
Laser Energy (J/ℓ-atm)	0.28	1.2
Discharge E/N (10^{-16} V-cm^2)	---	2.8
Electrical Efficiency (percent)	5.8	0.38
Chemical Efficiency (percent) ($H + Cl_2 \rightarrow HCl(V) + Cl$, ΔH = 45 kcal/mole)	0.22	0.94

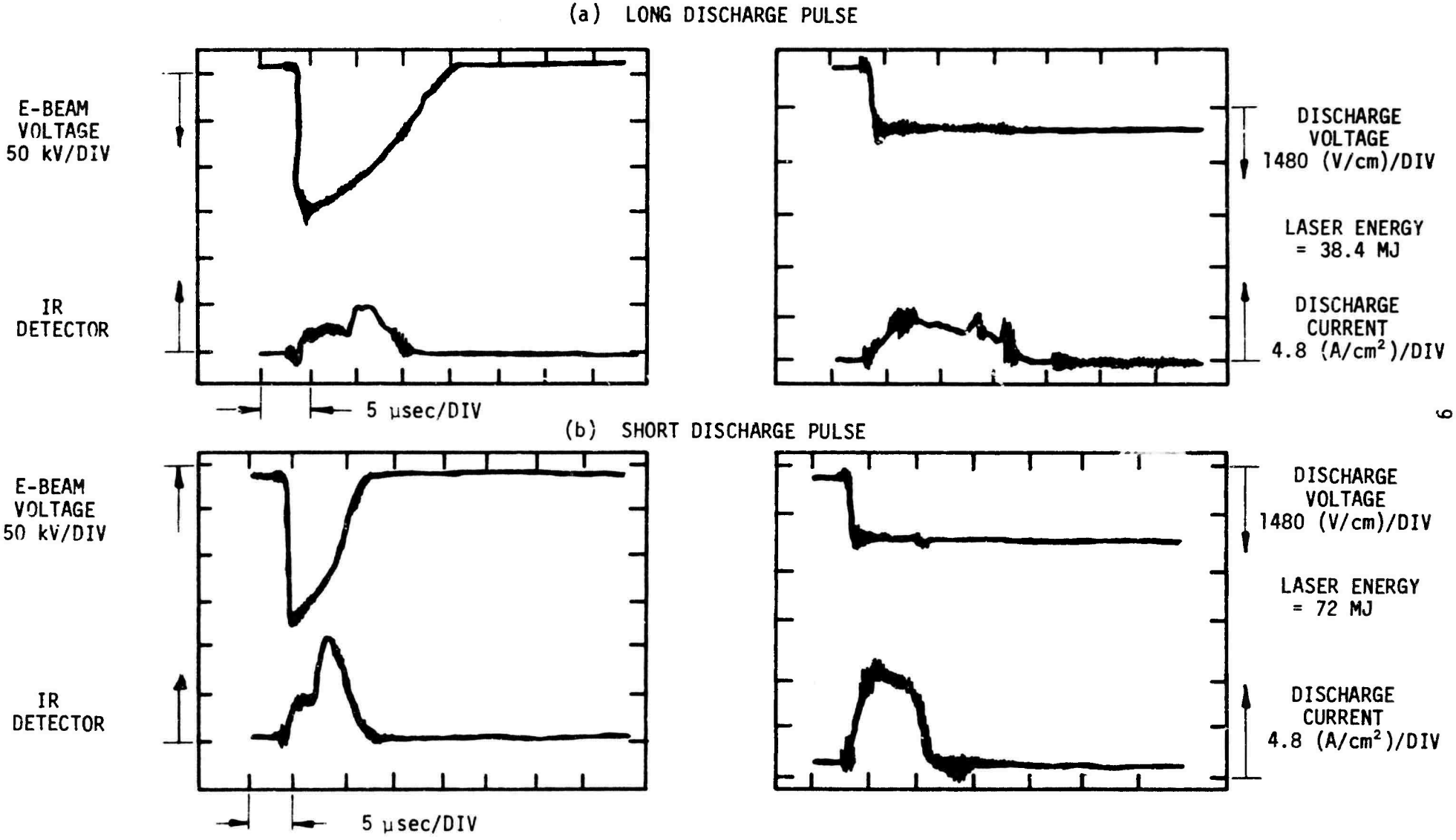

Figure 4. Variation of the Electron Beam Pulse Duration and Current Density and Its Effect on the HCl Laser Energy. The infrared detector trace shows a small early signal which is due to e-beam induced noise. Gas mixtures $Ar/H_2/Cl_2$ 49.2/49.2/1.5 at 200 torr total pressure.

the electrical efficiency using the discharge is 15 times worse than the e-beam alone case. The electron beam pulse length for the data of Table I was 5 μsec.

In the following three subsections (2.2.3, 2.2.4, and 2.2.5), specific parametric properties of the electrically excited HCl laser will be discussed. Gas composition as well as variations in the electrical properties of the discharge and e-beam were studied.

2.2.3. Discharge Pulse Duration Effects

Variation of the e-beam pulse length, hence the discharge duration, could be accomplished by changing the internal gun spacing, as described in Reference 1 and Figures 1 and 2. When the e-beam pulse duration was extended from 5 μsec to 10 μsec, the same total discharge energy could be deposited in the gas, since the discharge current density dropped by one-half for the longer pulse. However, the laser energy was found to double in the shorter discharge pulse case. Figure 4 illustrates the improvement in laser energy using the shorter duration, higher current e-beam configuration. The strong time dependence of the total energy input suggests that a rapid V-R,T deactivation process for HCl or H_2 may be occurring during the 10 μsec excitation pulse in Figure 4a. This hypothesis is also compatible with the observation that the laser signal intensity in Figures 4a and 4b has begun decreasing before the discharge pumping has ended.

A second possibility is related to thermalization of the HCl vibrational levels by the electrons. This effect has been observed in

electrically excited CO lasers (Ref. 2) where the laser gain significantly increases following the end of the discharge pulse. This effect would be more detrimental in the longer HCl electrical pulse case (Fig. 4a) than in the shorter pulse case (Fig. 4b), since in Figure 4b the laser pulse actually extends somewhat beyond the end of the discharge pulse. The electron "de-pumping" mechanism could be eliminated in a shorter (1 μsec) electrical pumping experiment, where the laser reaches threshold shortly after the end of the discharge pulse.

A third alternative explanation was discussed in Section 2.1 of this report and is related to the effect of discharge current spreading. Since the e-beam pulse duration variation shown in Figure 4 was produced by changing the internal gun spacing, greater e-beam divergence may cause reduced discharge current density. Hence, the measured total current, divided by the discharge anode area, may not be a valid derivation of the discharge current density for the conditions of Figure 4a. The computed discharge power input may therefore be smaller than that found by multiplying the discharge current density by the electric field gradient. Hence, the comparison of Figures 4a and 4b as equal discharge energy input cases may not be correct. An aperture will be inserted in future experiments to limit the e-beam and discharge spreading.

2.2.4. Chlorine Concentration Effects

Figure 5 illustrates the effect of increased chlorine fraction on the laser output and discharge current. (Fig. 5a is the same oscilloscope trace as Fig. 4b, and is reused here since it represents the same e-gun

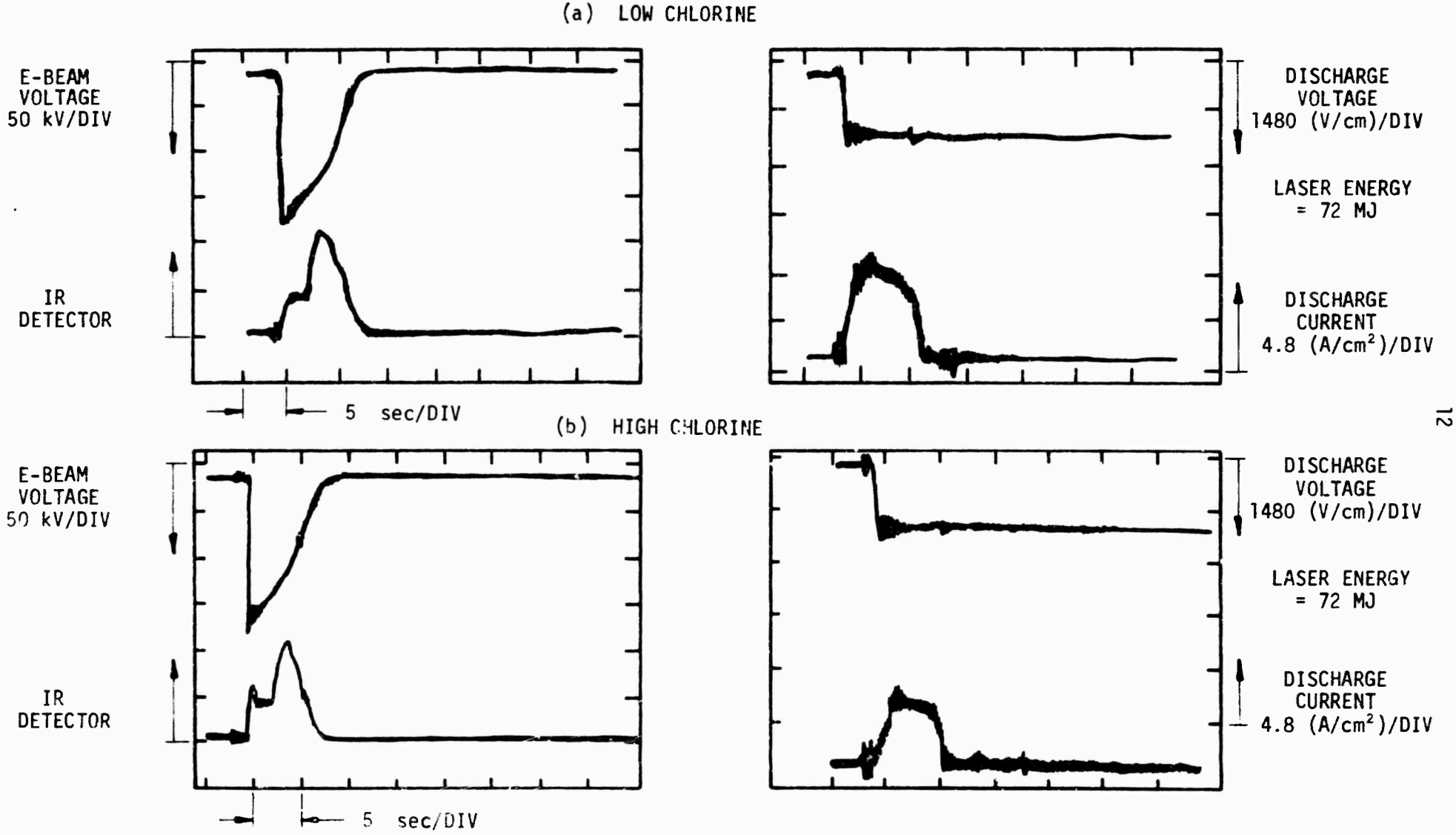

Figure 5. Variation of the Chlorine Mole Fraction and Its Effect on the Discharge and Laser Output. (a) $Ar/H_2/Cl_2$ 49.2/49.2/1.5, (b) $Ar/H_2/Cl_2$ 48.9/48.9/2.2. Total pressure 200 torr in both cases.

configuration spacing as Fig. 5b.) The chlorine concentration in Figure 5b is 1.5 times greater than Figure 5a; however, the argon and hydrogen concentrations are the same for both experiments. As expected for an attachment limited discharge, the discharge current in Figure 5b is two-thirds that of Figure 5a, since $\beta N_e N_{Cl_2}$ will remain constant for a fixed e-beam current source. Hence, the primary laser pumping reaction $H + Cl_2 \rightarrow HCl(V) + Cl$ will remain unchanged under the conditions of both Figures 5a and 5b, since as the Cl_2 concentration was raised by three-halves, the H atom production by the discharge drops by two-thirds due to the decreased energy deposited by the discharge. However, the key reaction of interest, $Cl + H_2^V \rightarrow H + HCl$, should have caused the laser energy to drop in Figure 5b since the H_2^V production also dropped by two-thirds. It is seen in Figure 5 that the laser energy was not altered by the change in the Cl_2 concentration. Unfortunately, this simple analysis ignores the reduced temperature rise for the conditions of Figure 5b and its effect on the laser gain. In addition, the H_2^V consumption rate by Cl atoms may be too slow under the present conditions to respond to a slight change in the H_2 vibrational temperature. Hence, it is difficult to draw a conclusion regarding the role of H_2^V in the laser kinetics using the present chlorine concentration dependence data.

2.2.5. Hydrogen Concentration Effects

The argon-hydrogen ratio was varied, keeping the total pressure (200 torr) and chlorine fraction (2 percent) constant. A summary of the results is presented in Table II. Argon fractions of 49 and 66 percent gave essentially the same laser output energy, which exceeded the best

Tab`e II

Variation in the Ratio of Argon to Hydrogen

	$Ar/H_2/Cl_2$			
	80/18/2	66/32/2	49/49/2	35/63/2
Laser Energy (mJ)	7.2	25.2	28.8	15.6
Discharge Energy Input (J/ℓ-atm)	181	231	231	296
Discharge E/N ($V\text{-}cm^2 \times 10^{16}$)	2.4	2.8	2.8	3.36

output obtainable with either the 80 or 35 percent argon mixtures. For this comparison, the electron gun was operated so that it gave a 10 μsec discharge pulse.

At the E/N values used in the initial survey experiments, significant H_2 dissociation can occur. The role of H_2^V in the laser kinetics must be studied at much lower E/N values than those presented in Table II. Ideally, experiments need to be performed at both high and low E/N values for various H_2 fractions, keeping the total electrical energy input constant. In this way, the relative importance of H atoms and H_2^V can be unravelled.

2.3. Calculated Laser Properties

Estimates for the H and Cl atom production, H_2 vibrational excitation, and discharge heating are given in Table III for the laser conditions of Table I. The Cl atom production is estimated by assuming that three chlorine atoms are produced for each ion pair created by the electron beam source (Ref. 3).

Estimates for the H atom production by the e-beam alone have been made by assuming that the excited argon metastables produced by ion-electron recombination lead to H_2 dissociation. The argon metastables excite the $a^3\Sigma_g^+$ state of H_2 which then radiates to the repulsive $b^3\Sigma_u^+$ state, creating H atoms. The H atom production rate by the electron beam could therefore equal twice the ion pair production rate, which is 4.7×10^{19} $(cm^3\text{-sec})^{-1}$ for an e-beam current density of 0.4 amps/cm^2. The hydrogen atom production by the e-beam probably accounts for the laser emission produced by the e-beam alone.

Table III

Calculated Laser Properties

Laser Gas Mixture $Ar/H_2/Cl_2$ 49/49/2; Discharge Energy Input-315 J/ℓ-atm; $E/N-2.8 \times 10^{-16}$ V-cm^2; E-Beam Current Density-0.4 A/cm^2

	E-BEAM	E-BEAM PLUS SUSTAINER
$[H_2(V)]/[H_2]$	---	0.15
$[H]/[H_2]$	2×10^{-4}	5×10^{-3}
$[Cl]/[Cl_2]$	8×10^{-3}	$\sim 8 \times 10^{-3}$
Temperature Rise (°K)	---	98

Boltzmann calculations for the power fraction of the discharge energy distributed into various excitation modes are presented in Figure 6. From this data, the vibrational excitation and dissociation fractions of H_2 given in Table III were computed. The gas temperature rise caused by the discharge pulse was assumed to be equal to the sum of the H_2 rotational and thermal excitation fractions. Production of atoms and vibrationally excited H_2 by the discharge (as well as the temperature rise) may be overestimated by approximately a factor of 2 due to discharge spreading, as discussed in Section 2.1.

Since the H atoms produced by the sustainer are essentially all consumed by the Cl_2 during the discharge pulse (5 μsec), the total Cl atom concentration at the end of the discharge is approximately 1.6×10^{16} cm^{-3}. Based on Wilkins' rate constants (see Section IV), the time constant for reaction of the H_2^V is approximately 4 μsec, which is comparable with the laser pulse duration (3 μsec) occurring during the 5 μsec discharge pulse. Hence, under the present discharge conditions, and based on these estimates, the Cl + H_2^V reaction could make some contribution to the laser pulse.

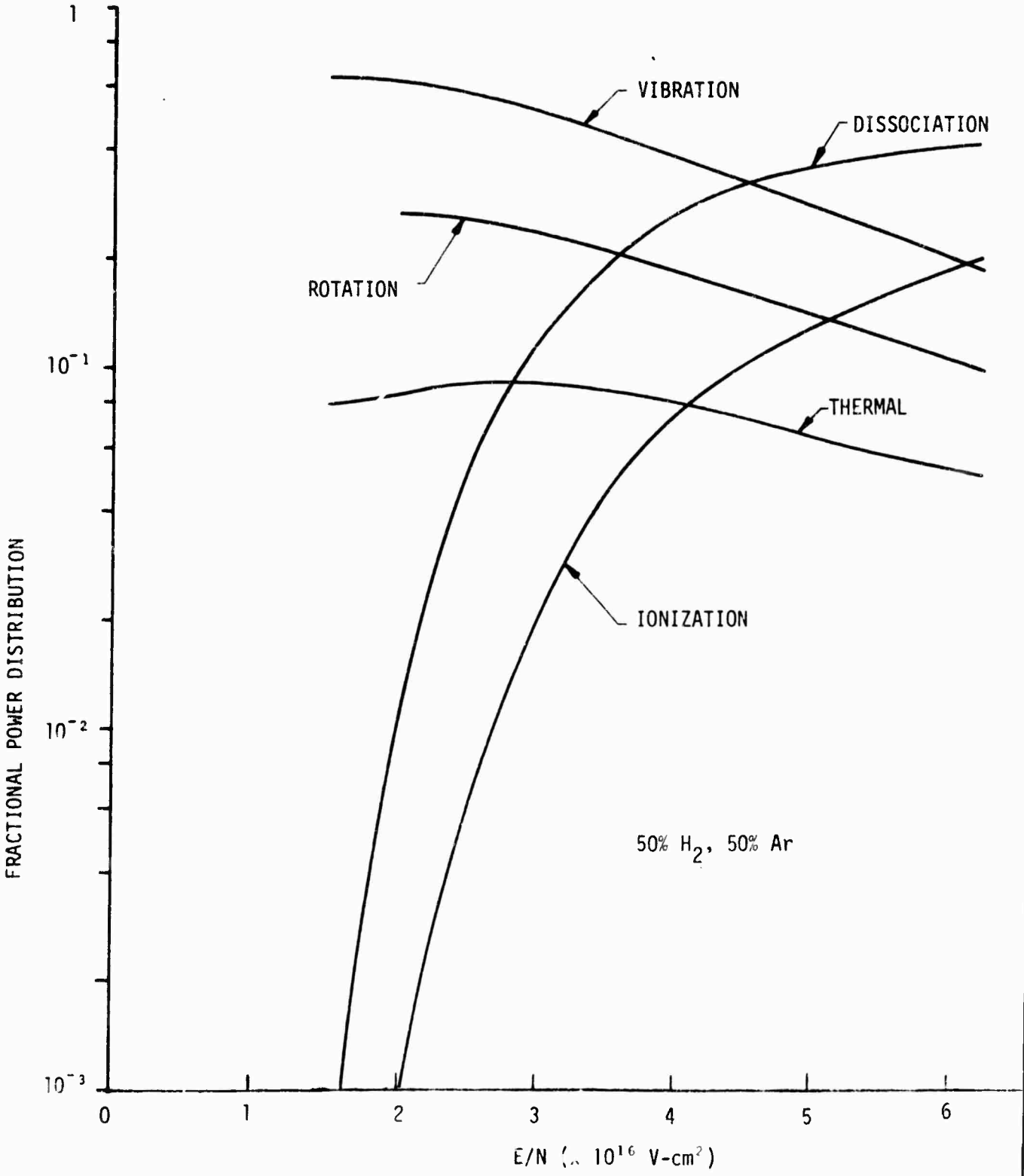

Figure 6. Boltzmann Calculation for an Argon/Hydrogen (50/50) Mixture

SECTION III

DIAGNOSTIC DEVELOPMENT

Three principal diagnostic methods were investigated in the present contract period: (1) Cl_2 monitor, (2) HCl probe laser, (3) coherent Anti-Stokes Raman spectroscopy (CARS) for H_2. The results obtained to date in each of these areas will be discussed in this section.

3.1 Chlorine Monitor

The continuum absorption of Cl_2 in the visible was used to detect small chlorine concentrations. Figure 7 shows the experimental setup for the Cl_2 measurements, which used a small Ultra Violet Products (Pen-Ray) Hg source and filter to isolate the 3650 Å Hg lines. The absorption coefficient of Cl_2 at this wavelength is 1.8×10^{-3} cm^{-1} $torr^{-1}$ (Ref. 4). A small monochromator (0.25 meter Jarrell-Ash) was also used to aid in discrimination against light emitted by e-beam and discharge excitation of the laser gas at wavelengths close to 3650 Å. A long folded path was also useful in discriminating against the uncollimated e-beam and sustainer light.

Figure 8 shows the time dependence of the Cl_2 absorption over a long period of time following the excitation pulse. The traces shown in Figure 8 are consistent with complete combustion of the Cl_2 in the excitation region of the e-beam.

The time regime of real interest for electrically excited HCl chemical laser is during and slightly after the actual discharge pulse, which is typically 5-10 μsec. Based on estimates of the Cl_2 dissociation rate by electrons and H atom reaction, only about 10-20 percent of the

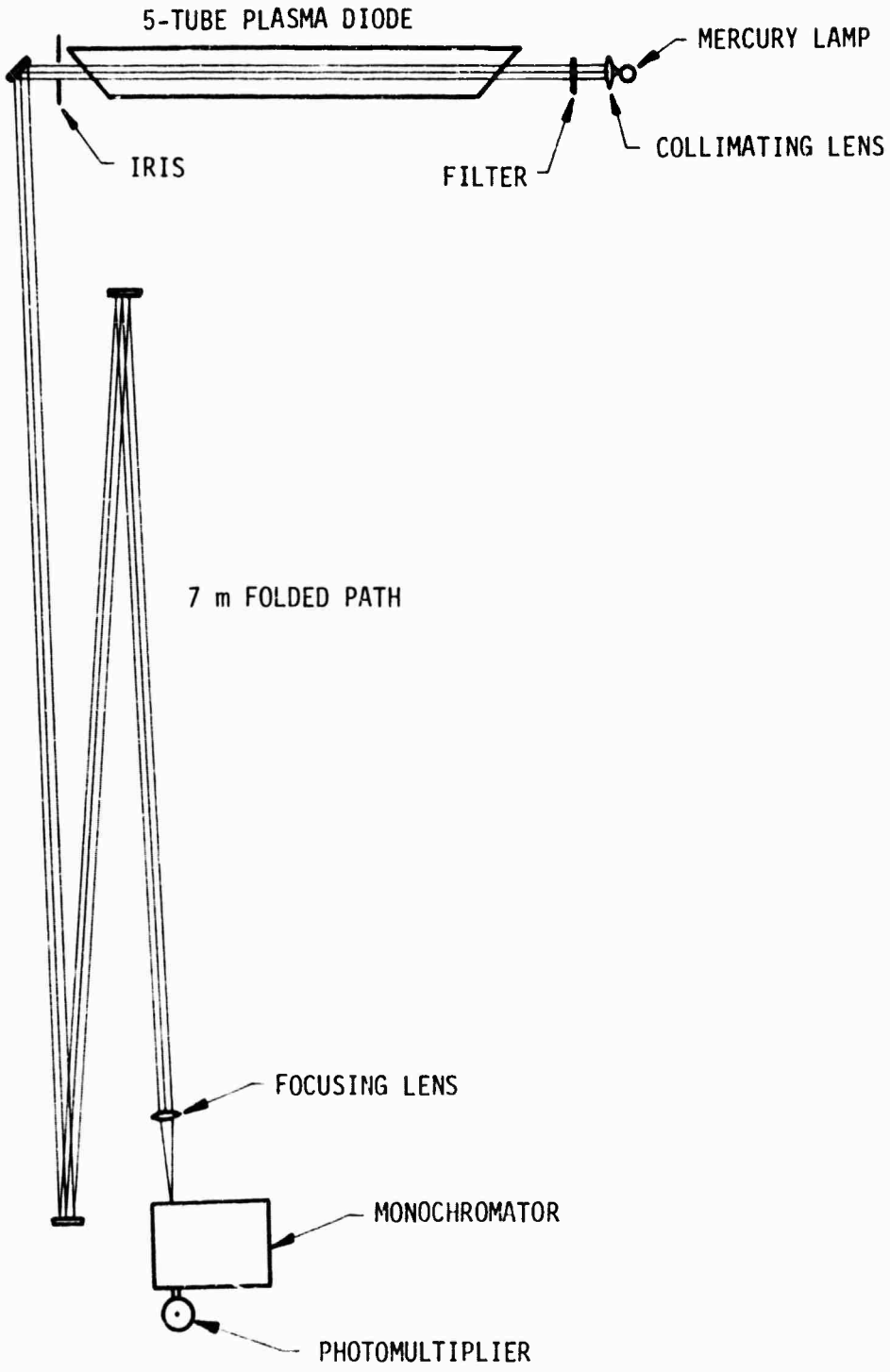

Figure 7. Experimental Set-Up for Cl_2 Concentration Monitor

76 00087

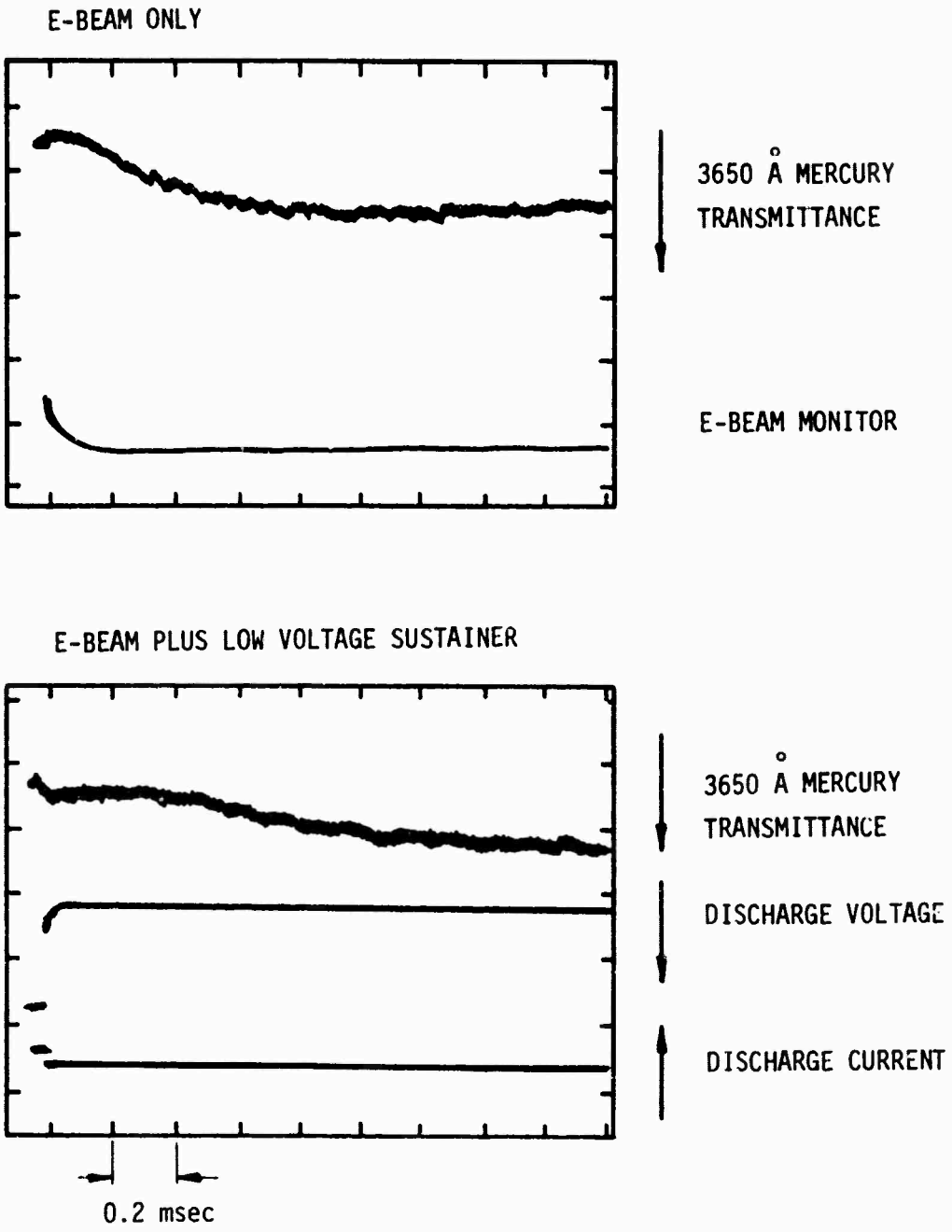

Figure 8. Cl_2 Absorption Measurements 200 Torr (49/49/2) $Ar/H_2/Cl_2$

76 00038

chlorine, under present conditions, is consumed on the short time scale of the laser. This means that a change in the Cl_2 absorption of only 3-5 percent, for the typical argon, hydrogen, chlorine (49/49/2) mixtures must be accurately measured. At present, this small change in absorption is too difficult to measure. A more stable, monochromatic light source such as a He-Cd laser would alleviate the dual problem of background emission from the discharge and source fluctuations common to normal arc lamps. An alternative solution consists of using a much brighter mercury arc lamp source, in a dual beam configuration to improve the baseline stability of the experiment. Both of these approaches will be investigated further in the next contract period.

3.2. HCl Probe Laser

A conventional chemical HCl pin laser has successfully been operated in mixtures of argon, hydrogen and chlorine. Typically only helium mixtures are used in chemical HCl and HF pin type discharge lasers (Ref. 5). The argon mixtures were lased in a line selected (grating) cavity at pressures up to 200 torr. Hence, argon induced line shifts of the HCl spectrum can be neglected when making gain and absorption measurements in e-beam stabilized discharges of argon, hydrogen, and chlorine mixtures.

3.3 CARS Measurements

Apparatus for the CARS measurement of vibrationally excited H_2 has been assembled and tested. The coherent signal will be much stronger than conventional Raman scattering and will be emitted in a very small solid angle determined by the focusing geometry. These characteristics

make the CARS technique very attractive as a diagnostic tool in luminous experimental environments, such as discharges, flames, shocks, etc. Previous work by Taran and co-workers (Ref. 6) has shown that quantitative H_2 gas concentration measurements could be made in flames using a Q-switched ruby laser and a high pressure H_2 stimulated Raman source. Recently, tunable dye lasers have been used to replace the fixed frequency limitations of the stimulated Raman scattering generator to study gases (Ref. 7) and liquids (Ref. 8). A CARS system capable of detecting a few torr of H_2 using a tunable dye laser has been constructed at MSNW and the following discussion presents details of the experimental arrangement and present detectivity limits of the apparatus.

Initial experiments in liquid benzene (Ref. 1) were quite successful and demonstrated the need for careful alignment of the ruby and dye laser sources so that they will cross at the required phase matching angle for benzene (1.2 degrees). Accurate dye laser wavelength adjustment was found to be a problem with the small 0.25 meter Jarrell-Ash monochromator and therefore a larger 0.5 meter monochromator was used in further experiments. In addition the ruby laser power had to be attenuated below the threshold for stimulated stokes scattering in benzene. Once the ruby and dye lasers were properly optimized (wavelength and alignment) the benzene CARS signal at 6496 Å was sufficiently intense so that it was visible on a white card in a darkened room.

Following the successful benzene experiments, slightly different optics were set-up to obtain CARS signals in H_2. Figure 9 is a schematic drawing of the optical arrangement used. The ruby laser consisted of a single ruby rod (3 in. long by 0.25 in. O.D.) pumped by two linear flashlamps

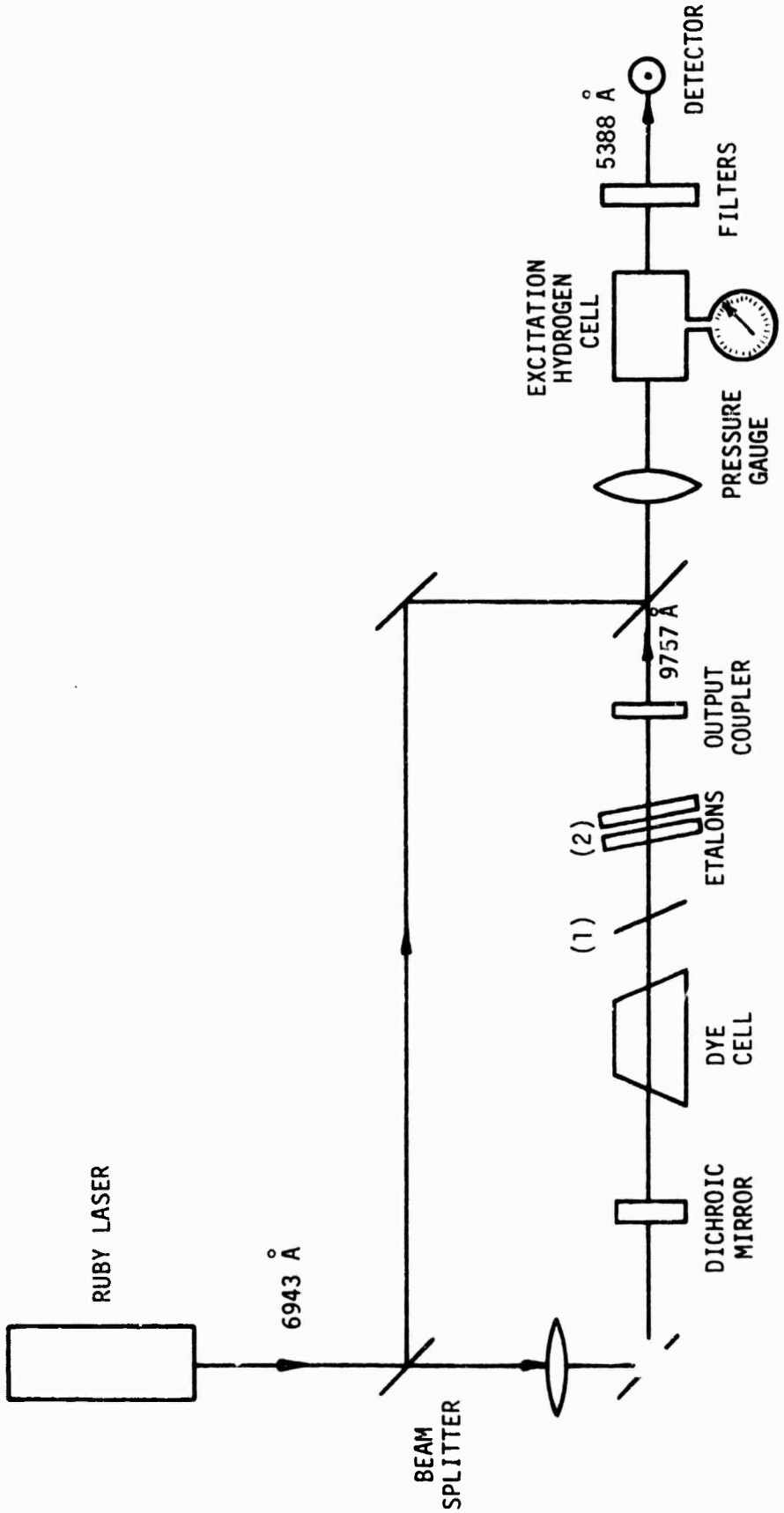

Figure 9. Schematic of Apparatus Used for Coherent Anti-Stokes Raman Emission by Four-Wave Mixing in Hydrogen

76 00089

in a double elliptical polished aluminum housing. A slow, dry nitrogen purge was used to provide cooling and prevent deterioration of the aluminum housing by ozone. Q-switching was accomplished using an electro-optic Pockel's cell. The rear cavity mirror was a totally reflecting 10 meter radius of curvature dielectric. A 66 percent resonant reflector consisting of two high index quartz flats was used as the output coupler. The ruby laser energy was split 2/3 and 1/3 by a beamsplitter and the smaller fraction used to pump a 3-cm dye cell containing acetone solutions of 1, 1´-Diethyl-4, 4´-quinotricarbocyanine iodide. The ruby laser was focused into the dye cell by a 50-cm focal length lens spaced 35 cm from the center of the dye cell.

Wavelength tuning was accomplished using the dual etalon scheme shown in Figure 7. Etalon (1) was a thin plastic membrane, 8 μm thick, coated on both sides for 70 percent reflectivity over the range 800 to 1000 nm, which would have a theoretical bandwidth of 2.0 nm. A narrow, air-gap Etalon reduced this width to approximately 0.1 nm. A small 9-in. focal length, achromatic lens focused the two co-linear laser beams into the H_2 sample cell. CARS emission was separated from the dye and ruby laser radiation by two green glass (Schott, VG-14) filters, and a IP28 photomultiplier detected the 538.8 nm anti-Stokes signal.

The co-linear nature of the optical arrangement greatly facilitated alignment of the two laser beams for spatial overlap, which we found to be rather difficult in a side-pumped, grating tuned cavity. In addition, ultra-narrow dye laser linewidths which would exactly match the H_2 Doppler width (0.003 nm) were not used in order to avoid extreme sensitivity of the

CARS signal to drifts in the dye laser frequency. This results in incomplete utilization of the dye power; however, further narrowing could result in reduced dye output which would nearly cancel any beneficial effect of reduced linewidth. No special efforts were made in these experiments to operate the ruby and dye lasers single mode. The repetition rate of the ruby laser was quite low (one shot/three to four minutes) due to the convection limited cooling of the ruby rod. A high repetition rate ruby or Nd:Yag laser would be a highly desirable feature to incorporate into certain experiments, since advantage could then be taken of signal averaging techniques. For the present experiments in pulsed discharges, which have an inherently low repetition rate, the low repetition rate ruby laser is not a limitation.

A detectivity limit of 15 torr H_2 was found in the present series of experiments. This is by no means an ultimate limit to the detectivity level. Improvements in the dye and ruby laser output powers would greatly reduce the minimum detection limit. Further measurements need to be made of the dye laser linewidth to determine whether the dye laser is operating with as narrow a linewidth as calculated from the etalon characteristics. Discrimination against the ruby light reaching the CARS detector also needs to be improved, and narrow band interference filters will be used in conjunction with the Schott glass filters.

SECTION IV

HCl CHEMICAL LASER COMPUTER MODEL

Basic data for an HCl chemical reaction laser model have been collected and a computer code is presently being written. Table IV contains the optical constants necessary for calculating the HCl laser gain. Table V contains a summary of the chemical reaction rate constants and vibrational decay rates for various constituents of the electrically excited gas mixture. The recent review of HCl rate constants by Bott and Cohen (Ref. 9) helped provide a critical evaluation of the data available in the literature. A Boltzmann code for calculating the fraction of the discharge energy distributed into the various H_2 channels (vibration, rotation, translation, electronic, and dissociation) will be used in conjunction with the chemical reaction code. Chlorine atom production will be found by equating the electron beam production rate of electrons with the attachment loss rate due to Cl_2. Direct electron pumping of HCl will be neglected in the initial calculations.

Since many of the crucial reaction rates (e.g., $H_2(V) + Cl \rightarrow HCl + H$) and deactivation rates (e.g., $HCl(V) + Cl \rightarrow HCl(V-1) + Cl$) have not been measured, computed values for these rates (Refs. 9, 10) will be used at first. Variation of these rates in the computer code will certainly be necessary to test the sensitivity of the HCl chemical laser model to these potentially critical rates.

Table IV

HCl OPTICAL CONSTANTS

Einstein A Coefficient

TRANSITION		$A(sec^{-1})$	$A_J(\text{P-branch}) = \left(\frac{J_{\text{lower level}}}{2J_{LL} - 1}\right) A$	REFERENCES
V=1	V=0	34.6		
V=2	V=1	59.4		11
V=3	V=2	74.7		
V=4	V=3	81.1		

Optical Broadening Cross Section in $(\text{Angstrom})^2$

P(J)-BRANCH	$Q_{HCl-HCl}$	Q_{HCl-Ar}	Q_{HCl-H_2}	REFERENCES
1	270	86.3	34.2	12
2	304	50.6	25.4	
3	302	45.8	19.2	13
4	296	37.6	15.0	
5	270	32.1	11.1	
6	220	27.1	10.6	
7	189	28.5	10.6	
8	161	18.8	11.0	
9	145			
10	130			
11	114			
12	97			
13	97			

TABLE V

Rate Coefficients (Note HCl(V) Level Involving Only V = 0 to 3)

Reaction	Rate Coefficient (cc/mole/sec)		References
1. $H+Cl_2 \underset{k_b}{\overset{k_f}{\rightleftharpoons}} HCl(V)+H$	$k_f = f(V) \times 5.7 \times 10^{13} e^{-\frac{1268}{T}}$	$f(0)=0$, $f(1)=.12$ $f(2)=.42$, $f(3)=.39$ $f(4)=.04$, $f(5)=.02$ $f(6)=.002$	14
2. $Cl+H_2(V) \underset{k_b}{\overset{k_f}{\rightleftharpoons}} HCl(V')+H$	$k_f = 4.8 \times 10^{13} e^{-\frac{2647}{T}}$	for V=V'=0	15
	$k_f = 1.29 \times 10^{14} T^{-.268} e^{-\frac{845}{T}}$	for V=1, V'=0	10
	$k_f = 2.83 \times 10^{15} T^{-.536} e^{-\frac{990}{T}}$	for V=1, V'=1	10
3. $HCl(V)+HCl(V') \underset{k_b}{\overset{k_f}{\rightleftharpoons}} HCl(V+1)+HCl(V'-1)$	$k_f = 8 \times 10^{14} T^{-1}$	V=V'=1	16,17
	$k_f = 1.6 \times 10^{15} T^{-1}$	V=2, V'=1	9
4. $HCl(V)+HCl \underset{k_b}{\overset{k_f}{\rightleftharpoons}} HCl(V-1)+HCl$	$k_f = V(1.6 \times 10^{17} T^{-3} + 8.7 \times 10^{4} T^{2})$		18

TABLE V, continued...

	Reaction	Rate Coefficient (cc/mole/sec)		References
5.	$HCl(V)+H_2 \underset{k_b}{\overset{k_f}{\rightleftharpoons}} HCl(V-1)+H_2$	$k_f = V(1 \times 10^{4}T^{2.23})$		9
6.	$HCl(V)+Cl_2 \underset{k_b}{\overset{k_f}{\rightleftharpoons}} HCl(V=1)+Cl_2$	$k_f = V\ (5 \times 10^{4}T^{2})$		19
7.	$HCl(V)+Ar \underset{k_b}{\overset{k_f}{\rightleftharpoons}} HCl(V-1)+Ar$	$k_f = V(7.8 \times 10^{-7}T^{5})$		20
8.	$HCl(V)+H \underset{k_b}{\overset{k_f}{\rightleftharpoons}} HCl(V')+H$	$*k_f = 6.16 \times 10^{14}T^{-.26}e^{-\frac{453}{T}}$	V=1, V'=0	10
		$*k_f = 4.57 \times 10^{14}T^{-.31}e^{-\frac{415}{T}}$	V=2, V'=1	
		$*k_f = 9.33 \times 10^{14}T^{-.36}e^{-\frac{440}{T}}$	V=2, V'=0	
		$*k_f = 1.66 \times 10^{15}T^{-.49}e^{-\frac{480}{T}}$	V=3, V'=2	
		$*k_f = 8.13 \times 10^{13}T^{-.14}e^{-\frac{322}{T}}$	V=3, V'=1	
		$*k_f = 6.6 \times 10^{14}T^{-.32}e^{-\frac{385}{T}}$	V=3, V'=0	

*Note: All of the above rates were scaled down by a factor of 3, as suggested by Bott ard Cohen, in order to come closer to agreement with the experimental data for V=1, V'=0.

TABLE V, continued...

	Reaction	Rate Coefficient (cc/mole/sec)		References
9.	$HCl(V)+Cl \underset{k_b}{\overset{k_f}{\rightleftharpoons}} HCl(V')+Cl$	$k_f = 5.6 \times 10^{13} T^{-.2} e^{-\frac{418}{T}}$	V=1, V'=0	21
		$k_f = 2.3 \times 10^{14} T^{-.37} e^{-\frac{490}{T}}$	V=2, V'=1	
		$k_f = 5.6 \times 10^{13} T^{-.28} e^{-\frac{510}{T}}$	V=2, V'=0	10
		$k_f = 5.5 \times 10^{14} T^{-.5} e^{-\frac{510}{T}}$	V-3, V'=2	
		$k_f = 2.3 \times 10^{14} T^{-.47} e^{-\frac{496}{T}}$	V=3, V'=1	
		$k_f = 5.6 \times 10^{13} T^{-.41} e^{-\frac{428}{T}}$	V=3, V'=0	
10.	$H_2(V=1)+H \rightarrow H_2(V=0)+H$	$k = 1.87 \times 10^{11}$ cc/mole/sec. @ 300 °K		22
11.	$Cl_2 + e \rightarrow 2\ Cl$	$k = 6 \times 10^{13}$ @ 300 °K		23
12.	$H_2(V=0) + e \rightarrow H_2(V=1) + e$			24
13.	$H_2(V=0) + e \rightarrow 2H + e$			24

SECTION V

SUMMARY OF RESULTS AND FUTURE PLANS

The present series of HCl laser experiments performed with the high current density (.2-.4 A/cm^2), long pulse (5-10 μsec) cold cathode electron beam source indicate that even higher electron beam current for a shorter duration would be desirable. Efficiency of electrical excitation is low (0.4 percent) at present, although six times better than the earlier plasma diode experiments. The electron gun will be slightly modified during the next contract period to allow higher current operation for a shorter time duration. Further parametric laser performance studies will be made in the revised e-beam device. Specifically, the laser performance as a function of pulse duration will be investigated: the E/N dependence over a large range [$1 - 3 \times 10^{-16}$ $V\text{-}cm^2$] will be determined, and the parametric dependence on e-beam current density, discharge energy input, gas composition and pressure will be studied.

The computer model will be completed shortly, which will allow comparisons to be made with experimental observations and predict fruitful directions for further experimental work. Predictions regarding the effect of hydrogen vibrational excitation on the laser performance will be compared with parametric measurements of the laser performance at different E/Ns, discharge energy input, gas composition and pressure.

Diagnostics for the measurement of HCl and H_2 have progressed to the point where they can be coupled to the discharge experiments. The HCl probe laser will be used to measure pre-reaction in the argon, hydrogen,

chlorine mixtures and gain (or absorption) during the discharge pulse. Measurements of H_2 vibrational excitation using the CARS equipment will be strongly emphasized following completion of the parametric laser performance studies. The Cl_2 monitoring scheme still needs to be improved to the point where relatively small changes in the Cl_2 concentration can be measured.

Output wavelengths of the HCl laser will be measured as a further means for comparison with the laser model. An approximate value for the gas temperature can be found from the J value of a vibrational transition with the largest intensity. The relative intensities of the different vibrational transitions will also provide a check on the laser model predictions.

REFERENCES

1. L. Y. Nelson and S. R. Byron, "Efficient High Energy HCl Chemical Laser," MSNW Semi-Annual Report No. 75-131-1 (April 15, 1975).

2. T. G. Jones and S. R. Byron, "Supersonic Continuous Wave Carbon Monoxide Discharge Laser Technology," MSNW Report No. 74-128-1 (December 1974).

3. J. Wilson, H. L. Chen, W. Fyfe, R. Taylor, R. Little and R. Lowell, J. Appl. Phys. 44, 5447 (1973).

4. J. G. Calvert and J. N. Pitts, Jr., Photochemistry, John Wiley and Sons, Inc., N.Y., p. 21, 184 (1966).

5. O. R. Wood and T. Y. Chang, Appl. Phys. Letters 20, 77 (1972).

6. P. Regnier, F. Moya and J. P. E. Taran, AIAA Journal 12, 826 (1974).

7. J. J. Barrett and R. F. Begley, Appl. Phys. Letters 27, 129 (1975).

8. A. B. Harvey and R. L. Byer, Appl. Phys. Letters 25, 387 (1974).

9. N. Cohen and J. F. Bott, TR-0075 (5530)-7, Aerospace Corporation, El Segundo (1975).

10. R. L. Wilkins, J. Chem. Phys. 63, 2963 (1975).

11. O. K. Herbelin and G. Emanuel, J. Chem. Phys. 60, 689 (1974).

12. W. S. Benedict, et al., Can. J. Phys. 34, 850 (1956).

13. H. Babrov, G. Ameer, W. Benesch, J. Chem. Phys. 33, 145 (1960).

14. K. G. Anlauf, et al., J. Chem. Phys. 57, 1561 (1972).

15. S. W. Benson, et al., Int. J. Chem. Kinetics 1, 29 (1969).

16. B. M. Hopkins and H. L. Chen, J. Chem. Phys. 57, 3816 (1972).

17. Y. Noter, I. Burak and A. Szoke, J. Chem. Phys. 59, 970 (1973).

18. P. F. Zittel and C. B. Moore, J. Chem. Phys. 75, 1079 (1971).

19. N. C. Craig and C. B. Moore, J. Chem. Phys. 75, 1622 (1971).

20. R. V. Steele, Jr. and C. B. Moore, J. Chem. Phys. 60, 2794 (1971).

21. R. G. MacDonald, C. B. Moore, I. W. M. Smith, F. J. Wodarczyk, J. Chem. Phys. 62, 2934 (1975); and, R. L. Wilkins, TR-0075 (5530)-11, Aerospace Corporation, El Segundo (1974).

22. R. E. Center (private communication).

23. Estimated from experimental discharge current density measurements.

24. Boltzmann solution for E/N, x_{H_2}, x_{Ar}.